Velocity analysis for plane-wave source migration using the finite-frequency sensitivity kernel

Hui Yang, Formerly University of California at Santa Cruz; presently LandOcean Energy Services Co., Ltd., Beijing, 100084, China.*
Xiao-Bi Xie, and Yaofeng He, IGPP, University of California at Santa Cruz, Santa Cruz, CA 95064, USA.

Summary

We derive the finite-frequency sensitivity kernel which relating the errors in migration velocity model to residual moveout in common image gathers obtained from plane-wave source prestack depth migration. The broadband sensitivity kernel is validated by the directly measured sensitivity map. Based on this kernel, we propose a new wave-equation migration velocity analysis approach particularly for plane-wave source migration. This method avoids the expensive local angle or offset decomposition. Numerical method based on the one-way propagator is designed to calculate the sensitivity kernel. Using a simple 2D synthetic data set, we demonstrate the potential application of this new method in migration velocity analysis.

Introduction

Wave-equation based short-record prestack depth migration (PSDM) is widely used in reflection seismology for imaging the complex subsurface structures. However, shot-record PSDM is usually less efficient. To overcome this disadvantage, the shot record can be converted into synthetic plane-wave source record for PSDM (Zhang, et al., 2005; Liu, et al., 2006; Stoffa, et al., 2006). The related migration velocity analysis (MVA) has been investigated by Ji (1997) based on the high frequency asymptotic method. Jiao et al. (2002) conducted residual velocity analysis for plane-wave migration using a local 1-D model. In general, the MVA is still dominated by the ray-based method which is inconsistent with the wave-equation PSDM.

The sensitivity of finite-frequency signal to velocity variation has been investigated and applied to seismic tomography (e.g., Luo and Schuster, 1991; Woodward, 1992; Vasco et al., 1995, Spetzler and Snieder, 2004; Sava and Biondi, 2004; De Hoop, et al., 2006; Jocker, et al., 2006; Fliedner and Bevc, 2008). Sava and Biondi (2004) tested the wave-equation MVA, and Sava and Vlad (2008) detailed its numerical implementation for zero-offset migration, survey-sinking migration and shot-profile migration. Xie and Yang (2007, 2008a, b) derived the sensitivity kernel which relating the observed residual moveout (RMO) in shot-index common image gather (CIG) to the velocity model errors and proposed a MVA for shot-gather migration.

In this paper, we derive the sensitivity kernel relating the RMO in surface plane-wave source CIG to errors in velocity models. We then validate this kernel and propose a novel velocity updating approach particularly for PSDM with synthetic surface plane-wave sources.

Sensitivity Kernel for Plane-Wave Source RMO

In a plane-wave source migration, the down-going wave $u_D(\mathbf{r};\mathbf{p},\omega)$ can be synthesized from individual shot responses $u_D(\mathbf{r};\mathbf{r}_S,\omega)$ through (e.g., Zhang, et al., 2005)

$$u_D(\mathbf{r};\mathbf{p},\omega)=\int u_D(\mathbf{r};\mathbf{r}_S,\omega)e^{i\omega\mathbf{p}\cdot\mathbf{r}_S}d\mathbf{r}_S\,, \qquad (1)$$

where $\mathbf{r}$ is the space location, $\mathbf{r}_S$ is the shot location, ω is the angular frequency, $\mathbf{p}=\hat{\mathbf{e}}_P\sin(\alpha_s)/\overline{v}_{0s}$ is the wave parameter vector of the synthetic plane-wave source, $\hat{\mathbf{e}}_P$ is a unit vector indicating the bearing direction of the plane wave source, α_s is the plane-wave take-off angle from vertical direction, and $\overline{v}_{0s}$ is the average near-surface velocity. Similarly, the up-going wave $u_U(\mathbf{r};\mathbf{p},\omega)$ from a reflector can be obtained from up-going waves of individual shots $u_U(\mathbf{r};\mathbf{r}_S,\omega)$ using the same phase delay

$$u_U(\mathbf{r};\mathbf{p},\omega)=\int u_U(\mathbf{r};\mathbf{r}_S,\omega)e^{i\omega\mathbf{p}\cdot\mathbf{r}_S}d\mathbf{r}_S\,. \qquad (2)$$

Note, although labeled with the parameter $\mathbf{p}$, the down-going wave u_D is a plane wave only at the surface. Both u_D and u_U are not plane waves in a general heterogeneous model.

Assuming we conduct the PSDM in an initial velocity model $v_0(\mathbf{r})$ which is sufficiently close to the true velocity model $v_T(\mathbf{r})$, the MVA is trying to determine the velocity difference $\delta v=v_T-v_0$ from the inconsistency of the depth image. The partial image obtained in the initial model v_0 for plane source $\mathbf{p}$ can be expressed as (e.g., Zhang et al. 2005)

$$I(\mathbf{r}_I,\mathbf{p},\omega)=\omega^2u_D^0(\mathbf{r}_I;\mathbf{p},\omega)u_U^0(\mathbf{r}_I;\mathbf{p},\omega)^*, \qquad (3)$$

where u_D^0 and u_U^0 are extrapolated down- and up-going wavefields in the initial model, the asterisk denotes the complex conjugate, $\mathbf{r}_I$ is the location of the image point. The information regarding the velocity error δv (which

Velocity analysis for plane-wave source migration

can also be seen as the unknown velocity perturbation related to v_0) is carried by down- and up-going waves entering the image as phase delay. Using Rytov approximation (e.g., Slaney, et al., 1984; Jocker, et al, 2006; Xie and Yang, 2008a), the phase delay can be expressed as

$$\delta\varphi(\mathbf{r}_I,\mathbf{p},\omega)=\mathrm{Im}\left\{\frac{U_D(\mathbf{r}_I;\mathbf{p},\omega)}{u_D^0(\mathbf{r}_I;\mathbf{p},\omega)}+\frac{U_U(\mathbf{r}_I;\mathbf{p},\omega)^*}{u_U^0(\mathbf{r}_I;\mathbf{p},\omega)^*}\right\}, \quad (4)$$

where U_D and U_U are scattered waves due to the unknown velocity perturbation δv. Based on the Born approximation, these scattered waves can be expressed as

$$U_D(\mathbf{r}_I;\mathbf{p},\omega)=2S(\omega)\int_V k_0^2 m(\mathbf{r}')G_D(\mathbf{r}';\mathbf{p},\omega)G(\mathbf{r}';\mathbf{r}_I,\omega)dV' \quad (5)$$

$$U_U(\mathbf{r}_I;\mathbf{p},\omega)^*=2S(\omega)\int_V k_0^2 m(\mathbf{r}')G_U(\mathbf{r}';\mathbf{p},\omega)^*G(\mathbf{r}';\mathbf{r}_I,\omega)dV' \quad (6)$$

where $m(\mathbf{r})=\delta v(\mathbf{r})/v_0(\mathbf{r})$ is the relative velocity perturbation, $k_0(\mathbf{r},\omega)=\omega/v_0(\mathbf{r})$ is the background wavenumber, $S(\omega)$ is the source spectrum, $G(\mathbf{r};\mathbf{r}_I,\omega)$ is the Green's function, $G_D(\mathbf{r};\mathbf{p},\omega)$ and $G_U(\mathbf{r};\mathbf{p},\omega)$ are plane-wave Green's functions defined by

$$u_D^0(\mathbf{r};\mathbf{p},\omega)=S(\omega)G_D(\mathbf{r};\mathbf{p},\omega), \quad (7)$$

$$u_U^0(\mathbf{r};\mathbf{p},\omega)=S(\omega)G_U(\mathbf{r};\mathbf{p},\omega). \quad (8)$$

All Green's functions are calculated in the initial model. The integral covers the entire space with velocity perturbations. Substituting equations 5-8 into 4, we have,

$$\delta\varphi(\mathbf{r}_I,\mathbf{p},\omega)=\int_V m(\mathbf{r}')K_D^F(\mathbf{r}',\mathbf{r}_I,\mathbf{p},\omega)dV' + \int_V m(\mathbf{r}')K_U^F(\mathbf{r}',\mathbf{r}_I,\mathbf{p},\omega)dV', \quad (9)$$

where

$$K_D^F(\mathbf{r},\mathbf{r}_I,\mathbf{p},\omega)=\mathrm{Im}\left[2k_0^2\frac{G_D(\mathbf{r};\mathbf{p},\omega)G(\mathbf{r};\mathbf{r}_I,\omega)}{G_D(\mathbf{r}_I;\mathbf{p},\omega)}\right], \quad (10)$$

and

$$K_U^F(\mathbf{r},\mathbf{r}_I,\mathbf{p},\omega)=\mathrm{Im}\left[2k_0^2\frac{G_U^*(\mathbf{r};\mathbf{p},\omega)G(\mathbf{r};\mathbf{r}_I,\omega)}{G_U^*(\mathbf{r}_I;\mathbf{p},\omega)}\right], \quad (11)$$

are single frequency sensitivity kernels or Fréchet kernels for the source and receiver sides. Equations 9-11 setup the relationship between the velocity perturbation and phase delay in the migrated image.

Following Xie and Yang (2008a), we can convert the phase delay $\delta\varphi$ into broadband traveltime delay δt,

$$\delta t(\mathbf{r}_I,\mathbf{p})=\int_V m(\mathbf{r}')K_D^B(\mathbf{r}',\mathbf{r}_I,\mathbf{p})dV' + \int_V m(\mathbf{r}')K_U^B(\mathbf{r}',\mathbf{r}_I,\mathbf{p})dV', \quad (12)$$

where

$$K_D^B(\mathbf{r},\mathbf{r}_I,\mathbf{p})=\int\frac{W(\omega)}{\omega}K_D^F(\mathbf{r},\mathbf{r}_I,\mathbf{p},\omega)d\omega, \quad (13)$$

$$K_U^B(\mathbf{r},\mathbf{r}_I,\mathbf{p})=\int\frac{W(\omega)}{\omega}K_U^F(\mathbf{r},\mathbf{r}_I,\mathbf{p},\omega)d\omega, \quad (14)$$

are broadband traveltime delay sensitivity kernels for the source and receiver side, and $W(\omega)$ is a weighting function (Xie and Yang, 2008a).

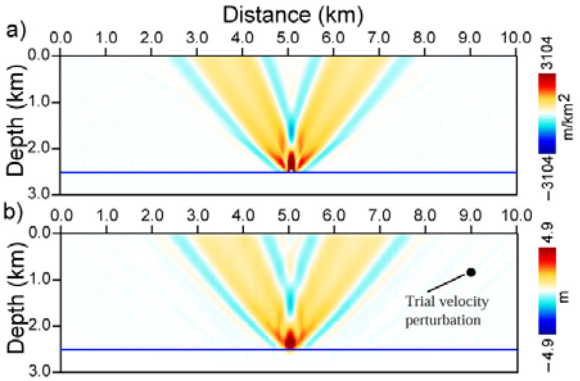

Figure. 1: Validation of sensitivity kernel for plane-wave source PSDM, where (a) is the theoretical sensitivity kernel and (b) is the sensitivity map directly measured from migration image. The trial perturbation, shown as a small solid circle in (b), has a diameter of 200 m and a velocity perturbation of 5%.

The traveltime delay can be further converted into the RMO in depth domain via (e.g., Stork, 1992; Xie and Yang, 2008a)

$$R(\mathbf{r}_I,\mathbf{p})=-A(\mathbf{r}_I,\mathbf{p})\delta t(\mathbf{r}_I,\mathbf{p}), \quad (15)$$

where

$$A(\mathbf{r}_I,\mathbf{p})=v_0(\mathbf{r}_I)/\left[2\cos\theta(\mathbf{r}_I,\mathbf{p})\cos\alpha(\mathbf{r}_I)\right], \quad (16)$$

where $\theta(\mathbf{r}_I,\mathbf{p})$ is the reflection angle relating to the reflector normal direction and $\alpha(\mathbf{r}_I)$ is the target dip angle at image point $\mathbf{r}_I$. Substituting equations 12-14 into equation 15, we finally have the relationship between the velocity perturbation δv and the RMO in depth image. The correspondent sensitivity kernel 13-14 is for CIGs indexed by the plane-wave source $\mathbf{p}$.

Validation of Theoretical Sensitivity Kernel

To validate the theoretical formulation, we compare the sensitivity kernel calculated from equations 12-16 with the directly measured sensitivity map. Shown in Fig. 1a is the broadband theoretical kernel calculated in a 2D model which has a constant background velocity of 3.5 km/s and a horizontal reflector located at depth 2.5 km. The synthetic plane-wave source has an incident angle of 30° and a 17.5

Velocity analysis for plane-wave source migration

Hz Ricker wavelet. The image point is located at distance 5.0 km. A one-way generalized screen propagator based on the multiple-forward scattering and single back-scattering approximation (Xie and Wu, 2001; Wu et al. 2006) is used to calculate the broadband sensitivity kernel. Fig. 1b shows the sensitivity map directly measured from plane-wave PSDM imaging. The method has been detailed in Xie and Yang (2008a). The general consistency between these sensitivity kernels verifies the theory and algorithm.

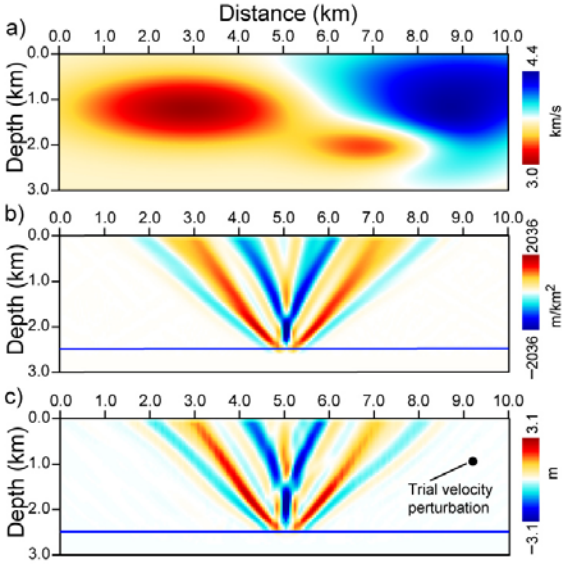

Figure 2: Comparison of differential sensitivity kernels in a heterogeneous background model, with (a) the velocity model, (b) the theoretically calculated differential kernel, and (c) the measured sensitivity map. The take-off angles of the two plane-wave sources are 45° and 30°, respectively.

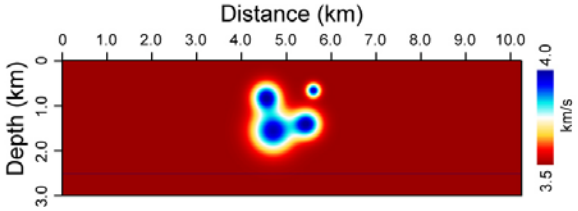

Figure 3: Velocity model used to test the MVA.

Inversion System

In practice, the absolute RMO is usually unavailable. Instead, MVA often adopts the degree of alignment of different experiments within the same CIG to judge the migration velocity model. The best alignment of events can be achieved by minimizing the relative RMO

$$\delta R(\mathbf{r}_I,\mathbf{p}_1,\mathbf{p}_2) = R(\mathbf{r}_I,\mathbf{p}_2) - R(\mathbf{r}_I,\mathbf{p}_1)\ . \quad (17)$$

Substituting equations 12-16 into equation 17, δR can be expressed as:

$$\delta R(\mathbf{r}_I,\mathbf{p}_1,\mathbf{p}_2) = -\int_V m(\mathbf{r}')\,K^B(\mathbf{r}',\mathbf{r}_I,\mathbf{p}_1,\mathbf{p}_2)\,dV', \quad (18)$$

where,

$$K^B(\mathbf{r},\mathbf{r}_I,\mathbf{p}_1,\mathbf{p}_2) = A(\mathbf{r}_I,\mathbf{p}_2)\left[K_D^B(\mathbf{r},\mathbf{r}_I,\mathbf{p}_2) - K_U^B(\mathbf{r},\mathbf{r}_I,\mathbf{p}_2)\right] - A(\mathbf{r}_I,\mathbf{p}_1)\left[K_D^B(\mathbf{r},\mathbf{r}_I,\mathbf{p}_1) - K_U^B(\mathbf{r},\mathbf{r}_I,\mathbf{p}_1)\right], \quad (19)$$

is the broadband differential sensitivity kernel which combines kernels from a pair of plane-wave parameters $\mathbf{p}_1$ and $\mathbf{p}_2$ within the same CIG. Equations 18 and 19 form the inversion system for the perturbation $m(\mathbf{r})$ which will be used to update the initial velocity model. Illustrated in Fig. 2 are differential sensitivity kernels in a 2D model, where 2a is the heterogeneous velocity model, 2b is the theoretically calculated differential sensitivity kernel using equation 19 and a pair of plane waves of 45° and 30°, and 2c is the directly measured sensitivity map. In general, Figs. 2b and 2c have the similar pattern.

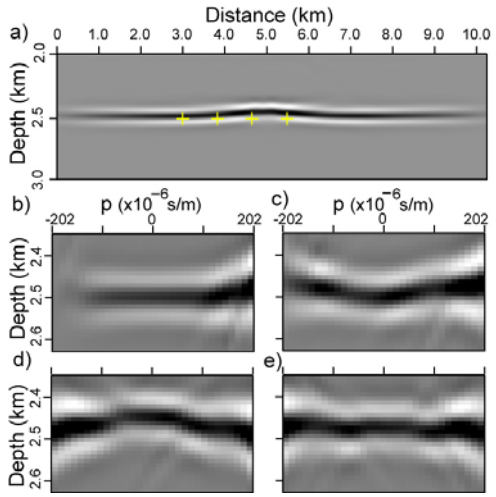

Figure 4: Result from plane-wave source migration in the initial model, with (a) stacked image, and (b)–(e) CIGs at selected image points indicated by crosses in (a).

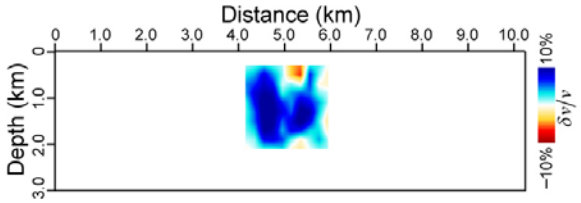

Figure 5: Inverted velocity perturbations.

Numerical Example

Illustrated in Fig. 3 is a simple model adopted to demonstrate the potential applications of the plane-source sensitivity kernel in MVA. The velocity model is composed

Velocity analysis for plane-wave source migration

of a 3.5 km/s constant background velocity and four patches of velocity perturbations in the middle of the model. The velocity perturbation in each patch is Gaussian distributed with its perturbation at the center is 10%. Their different sizes are used to test the inversion resolution. A horizontal reflector is located at depth 2.5 km. Shot gather records with full acquisition aperture are synthesized using a fourth-order scalar wave finite-difference method. Using equations 1-2 and taking $|\alpha_s| = 45^\circ$, we compose the shot gathers into 31 surface plane-waves, which are equally distributed in p values.

Using a one-way wave equation based method (Wu, et al., 2008), we first conduct the plane-wave source PSDM in the background model. Shown in Fig. 4a is the resulted image, and in 4b to 4e are CIGs at selected image points. The apparent RMOs in these CIGs are evidence of existing velocity errors. The CIGs collected from 31 evenly distributed image points are used as data. The sensitivity kernels are calculated for these image points. The dip angles are estimated from the image and reflection angles are from kernel calculations using the method of Xie and Wu (2002). Finally, we use the least-squares method of Lawson and Hanson (1974) to solve the linear system 18.

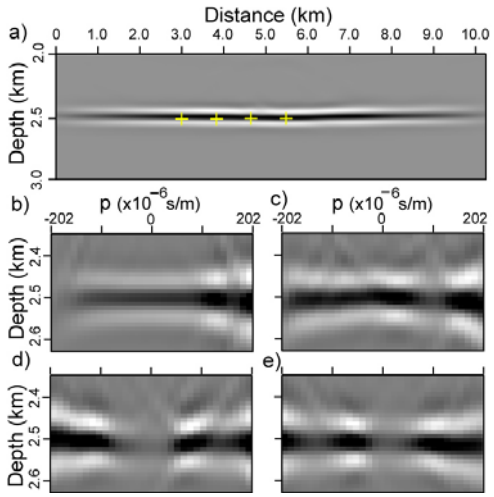

Figure 6: Similar to Fig. 4, except the result is obtained from the updated velocity model.

For simplicity, we limit the inversion in an 1.5×1.5-km square with the rest of the model unperturbed. A 6×6 grid is used to control the inversion. Within the grid, a bi-linear function is used to interpolate the model. For details of the model partitioning and kernel storing, see Xie and Yang (2008b). Shown in Fig. 5 is the inverted velocity perturbation which is very close to the original velocity perturbation in Fig. 3 and is used to correct the initial model. The migration is then conducted in the updated model. The result is shown in Fig. 6a and the CIGs are in 6b-6e. Comparing to Fig. 4, both the image and the CIGs are flattened. As a comparison, shown in Fig. 7 is the migrated result using the true velocity model. The CIGs in Figs. 6 and 7 are very similar, indicating the velocity model is considerably improved through the updating process.

Conclusions and Discussions

The finite-frequency sensitivity kernel is derived for the CIGs indexed by surface plane-wave parameters. Based on this sensitivity kernel, a novel wave-equation migration velocity analysis approach is proposed for surface plane-wave source PSDM. Numerical model demonstrates the potential application of this method. Since the kernel is formulated for surface plane-wave CIG, no expensive local angle or offset decomposition is required. The current numerical test is close to the linear condition. If the initial model is considerably biased from the object model, the nonlinear effect will become apparent and iterations should be required. The current numerical example is for a 2D model. However, there is no major obstacle to generalize this method to 3D problems.

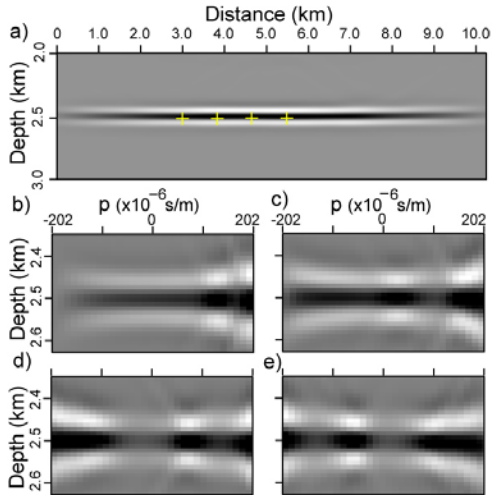

Figure 7: Similar to Fig. 4, except the result is obtained from the true velocity model.

Acknowledgments

This research is supported by the WTOPI Research Consortium at the University of California, Santa Cruz. One of us, Hui Yang, wishes to thank the support from LandOcean Energy Services Co., Ltd., during the preparation of this manuscript.

EDITED REFERENCES

Note: This reference list is a copy-edited version of the reference list submitted by the author. Reference lists for the 2009 SEG Technical Program Expanded Abstracts have been copy edited so that references provided with the online metadata for each paper will achieve a high degree of linking to cited sources that appear on the Web.

REFERENCES

de Hoop, M. V., R. D. van der Hilst, and P. Shen, 2006, Wave equation reflection tomography: annihilators and sensitivity kernels: Geophysical Journal International, **167**, 1332–1352.

Fliedner M., and D. Bevc, 2008, Automated velocity-model building with wavepath tomography: Geophysics, **73**, no. 5, VE195–VE204.

Ji, J., 1997, Tomographic velocity estimation with plane-wave synthesis: Geophysics, **62**, 1825–1838.

Jiao, J., P. L. Stoffa, M. K. Sen, and R. K. Seifoullaev, 2002, Residual migration-velocity analysis in the plane-wave domain: Geophysics, **67**, 1258–1269.

Jocker, J., J. Spetzler, D. Smeulders, and J. Trampert, 2006, Validation of first-order diffraction theory for the traveltimes and amplitudes of propagating waves: Geophysics, **71**, no. 6, T167–T177.

Lawson, C. L., and R. J. Hanson, 1974, Solving least squares problems: Prentice-Hall, Inc.

Liu, F., D. W. Hanson, N. D. Whitmore, R. S. Day, and R. H. Stolt, 2006, Toward a unified analysis for source plane-wave migration: Geophysics, **71**, no. 4, S129–S139.

Luo, Y., and G. T. Schuster, 1991, Wave-equation traveltime tomography: Geophysics, **56**, 645–653.

Sava, P. C., and B. Biondi, 2004, Wave-equation migration velocity analysis - I: Theory: Geophysical Prospecting, **52**, 593–606.

Sava, P., and I. Vlad, 2008, Numeric implementation of wave-equation migration velocity analysis operators: Geophysics, **73**, no. 5, VE145–VE159.

Slaney, M., A. C., Kak, and L. E., Larsen, 1984, Limitations of imaging with first-order diffraction tomography: Institute of Electrical and Electronics Engineers, Transactions on Microwave Theory and Techniques, **32**, 860–873.

Spetzler, J., and R. Snieder, 2004, The Fresnel volume and transmitted waves: Geophysics, **69**, 653–663.

Stoffa, P. L., M. K. Sen, R. K. Seifoullaev, R. C. Pestana, and J. T. Fokkema, 2006, Plane-wave depth migration: Geophysics, **71**, no. 6, S261–S272.

Stork, C., 1992, Reflection tomography in the postmigrated domain: Geophysics, **57**, 680–692.

Vasco, D. W., J. E. Peterson, Jr., and E. L. Majer, 1995, Beyond ray tomography: Wavepaths and Fresnel volumes: Geophysics, **60**, 1790–1804.

Woodward, M. J., 1992, Wave-equation tomography: Geophysics, **57**, 15–26.

Wu, R. S., X. B. Xie, and X. Y. Wu, 2006, One-way and one-return approximations (de Wolf approximation) for fast elastic wave modeling in complex media, *in* R. S. Wu and V. Maupin, eds., Advances in wave propagation in heterogeneous earth: Elsevier, 265–322.

Wu, R. S., Y. Z. Wang, and M. Q. Luo, 2008, Beamlet migration using local cosine basis, Geophysics **73**, no. 5, S207–-S217.

Xie, X. B., and R. S. Wu, 2001, Modeling elastic wave forward propagation and reflection using the complex screen method: Journal of the Acoustical Society of America, **109**, 2629–2635.

———, 2002, Extracting angle domain information from migrated wavefield: 72nd Annual International Meeting, SEG, Expanded Abstracts, 1360–1363.

Xie, X. B., and H. Yang, 2007, A migration-velocity updating method based on the shot-index common image gather and finite-frequency sensitivity kernel: 77th Annual International Meeting, SEG, Expanded Abstracts, 2767–2771.

———, 2008a, The finite-frequency sensitivity kernel for migration residual moveout and its applications in migration velocity analysis: Geophysics, **73**, no. 6, S241–S249.

———, 2008b, A wave-equation migration velocity analysis approach based on the finite-frequency sensitivity kernel: 78th Annual International Meeting, SEG, Expanded Abstracts, 3093–3097.

Zhang, Y., J. Sun, C. Notfors, S. H. Gray, L. Chernis, and J. Young, 2005, Delayed-shot 3D depth migration: Geophysics, **70**, no. 5, E21–E28.